HHS Public Access

Author manuscript

Solid State Nucl Magn Reson. Author manuscript; available in PMC 2017 June 01.

Published in final edited form as:

Solid State Nucl Magn Reson. 2016 ; 76-77: 1–6. doi:10.1016/j.ssnmr.2016.03.001.

Proton-detected 3D $^{15}N/^{1}H/^{1}H$ isotropic/anisotropic/isotropic chemical shift correlation solid-state NMR at 70 kHz MAS

Manoj Kumar Pandey[a], **Jayasubba Reddy Yarava**[a,1], **Rongchun Zhang**[b], **Ayyalusamy Ramamoorthy**[b], and **Yusuke Nishiyama**[a,c,*]

[a]RIKEN CLST-JEOL Collaboration Center, Yokohama, Kanagawa 230-0045, Japan

[b]Biophysics and Department of Chemistry, University of Michigan, Ann Arbor, MI 48109-1055, USA

[c]JEOL RESONANCE Inc., Musashino, Akishima, Tokyo 196-8558, Japan

Abstract

Chemical shift anisotropy (CSA) tensors offer a wealth of information for structural and dynamics studies of a variety of chemical and biological systems. In particular, CSA of amide protons can provide piercing insights into hydrogen-bonding interactions that vary with the backbone conformation of a protein and dynamics. However, the narrow span of amide proton resonances makes it very difficult to measure ^{1}H CSAs of proteins even by using the recently proposed 2D $^{1}H/^{1}H$ anisotropic/isotropic chemical shift (CSA/CS) correlation technique. Such difficulties due to overlapping proton resonances can in general be overcome by utilizing the broad span of isotropic chemical shifts of low-gamma nuclei like ^{15}N. In this context, we demonstrate a proton-detected 3D $^{15}N/^{1}H/^{1}H$ CS/CSA/CS correlation experiment at fast MAS frequency (70 kHz) to measure ^{1}H CSA values of unresolved amide protons of N-acetyl-^{15}N-L-valyl-^{15}N-L-leucine (NAVL).

Graphical abstract

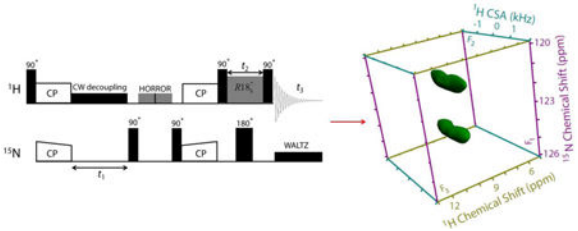

*Correspondence should be addressed (yunishiy@jeol.co.jp).

[1]Present address: Institut des Sciences et Ingénierie Chimiques, Ecole Polytechnique Fédérale de Lausanne (EPFL), CH-1015 Lausanne, Switzerland

Keywords

solid-state NMR; ultrafast MAS; 1H CSA; amide proton; 3D NMR; peptide; 1H detection

Introduction

Chemical shift anisotropy (CSA) tensors measured using solution and solid-state NMR methods have always played a pivotal role in getting deeper insights into inter and intra molecular H-bonding, electrostatic, and π-electron interactions.[1-12] All these interactions heavily rely on the relative position of protons with respect to each other and/or other atoms. Subsequently, measurement of ^{1}H CSA has been of considerable interest in various research groups.[13-20] In particular, amide protons (NH) are mostly involved in H-bonding interactions providing structural strength to enormous chemical and biological systems and, consequently, ^{1}H CSA which is extremely sensitive to the local electronic environment and dynamics can lead to a comprehensive understanding of these interactions. In general, ^{15}N isotropic/anisotropic chemical shifts of amide groups[11,21,22] are used to study H-bonding interactions. Since ^{15}N nuclei indirectly participate in H-bonding interactions, therefore measurement of ^{1}H isotropic/anisotropic chemical shifts of amide protons that are directly involved in H-bonding is of a greater significance. Nevertheless, the distribution of isotropic chemical shift of amide protons is rather limited and its relationship with the strength of H-bonding interaction is not so obvious. This brings a strong motivation to develop methods to measure ^{1}H CSA of H-bonded amide protons.

Usually, the determination of ^{1}H CSA has always been challenging due to its small size and the presence of strong homonuclear dipolar interactions between ^{1}Hs. In the past several methods using rotor-synchronous pulse sequences are reported that work well for its extraction either at slow magic angle spinning (MAS) or fast MAS. In a previous report, site-resolved ^{1}H CSA measurement of amide protons in proteins is already demonstrated through ^{13}C-detected 3D ^{1}H/^{15}N/^{13}C CSA/CS/CS experiment at a moderate MAS rate of 14 kHz.[15] Herein, the overlapped ^{1}H resonances were resolved in the ^{15}N/^{13}C dimensions, allowing a site specific determination of ^{1}H CSA of amide groups. While ^{1}H CSA can be measured at moderate MAS rates, the development of methods for its measurement at fast MAS (> 60 kHz)[18] are essential in order to avoid complexities associated with the experimental setup at slow MAS. Recently we demonstrated a 2D ^{1}H/^{1}H CSA/CS correlation method utilizing fast MAS and composite-180° pulse-based rotor-synchronized γ-encoded CSA recoupling sequences that result in undistorted ^{1}H CSA lineshapes with excellent efficiency.[23] In continuation to this, we also presented a 3D ^{1}H/^{1}H/^{1}H CSA/CSA/CS correlation experiment mediated through ^{1}H/^{1}H radio frequency-driven recoupling (RFDR) to extract relative orientation between two interacting ^{1}H CSA tensors at fast MAS.[24] However, 2D ^{1}H/^{1}H CSA/CS experiment cannot be utilized for CSA measurements of amide protons due to the lack of resolution in the ^{1}H CS dimension. In this regard, we present a 3D ^{15}N/^{1}H/^{1}H CS/CSA/CS correlation experiment on N-acetyl-^{15}N-L-valyl-^{15}N-L-leucine (NAVL) that results in site-resolved ^{1}H CSAs measured through ^{15}N isotropic chemical shifts. Manifold benefits of the 3D ^{1}H CSA measurement at fast MAS include: 1) enhanced sensitivity by ^{1}H detection,[25-37] 2) requirement of a tiny amount (0.3 –

1 mg) of sample due to small rotor volume (micro-coil probe design),[38-44] 3) direct correlation between ^{1}H CSA and ^{1}H CS which otherwise cannot be obtained due to overlap of ^{1}H CS resonances, 4) efficient and robust ^{1}H CSA recoupling,[23,24,45] and 5) low-power sequences can be implemented to avoid sample heating.[46-50]

Pulse sequence

The pulse sequence used for the proton-detected 3D ^{15}N/^{1}H/^{1}H CS/CSA/CS correlation experiment is shown in Figure 1. ^{1}H magnetization is transferred to ^{15}N nuclei using ramped-amplitude cross-polarization (RAMP-CP).[51] After which ^{15}N nuclei are allowed to evolve during t_1 under their isotropic chemical shifts in the presence of ^{15}N-^{1}H heteronuclear low-power CW decoupling on the ^{1}H channel. ^{15}N magnetization is then back transferred to ^{1}H by the second RAMP-CP. Residual ^{1}H transverse magnetization is removed by the use of the homonuclear rotary resonance (HORROR) sequence[52-54] on the ^{1}H channel just before the application of second CP.[55] While the ^{15}N magnetization is stored along the z-axis by the first 90° pulse on ^{15}N just before the HORROR irradiation to avoid time-evolution and transversal relaxation, the second 90° pulse on ^{15}N prepares magnetization for the second CP step. ^{1}H magnetization is stored along the z-axis by the use of a 90° pulse just after the second CP step and is allowed to evolve under the recoupled ^{1}H CSA using the symmetry-based $R18_8^7(270^\circ 90^\circ)$ sequence with the composite-180° pulse element during the t_2 period.[23] A 180° pulse in the middle of CSA recoupling period (t_2) is applied on the ^{15}N channel to decouple ^{15}N-^{1}H hetronuclear couplings in contrast to the previously reported pulse sequences wherein 180° pulses are applied in the middle of every cycle time of the CSA recoupling pulses.[15-17,56] Finally, ^{1}H magnetization is prepared for detection by the application of a 90° read pulse and data is acquired in the presence of ^{15}N-^{1}H WALTZ decoupling on the ^{15}N channel. While the States-TPPI (Time Proportional Phase Incrementation)[57] approach is applied to the t_1 period to obtain pure absorption line shape, the amplitude modulated signals are recorded in the t_2 period.

Experimental

All NMR measurements were carried out at a 600 MHz solid-state NMR spectrometer (JEOL RESONANCE Inc., JNM-ECZ600R) equipped with a 0.75 mm double-resonance ultrafast MAS probe (JEOL RESONANCE Inc.) operating at ^{1}H and ^{15}N Larmor frequencies of 599.67 MHz and 60.76 MHz, respectively. Approximately 0.3 mg of NAVL was packed into a 0.75 mm zirconia rotor and all data were collected at an ambient temperature under 70 kHz MAS. The ^{1}H and ^{15}N 90° pulse lengths were set to 0.6 and 1.4 μs, respectively. A recycle delay of 5 s and an acquisition time of 8.19 ms were used in the 3D experiment. 8 transients were coadded for each 32 t_1 and t_2 increments. While a longer contact time of 4 ms was used for the first CP (^{1}H to ^{15}N) to maximize the magnetization transfer efficiency from protons to ^{15}N nuclei, a short contact time of 0.4 ms was used for the second CP (^{15}N to ^{1}H) to select only those protons that are directly bonded to nitrogens in NAVL. The double quantum CP condition in both CP steps was achieved using 15 and 55 kHz RF field strengths for ^{1}H and ^{15}N, respectively.[47,49,50,58] The use of double quantum CP condition becomes essential especially for heat-sensitive samples like proteins to avoid sample degradation due to rf heating during the experiment. However, such matching

condition can be sensitive to chemical shift offsets due to the limited rf power. In the present study as the ^{1}H chemical shift range of amide groups is limited, we used a weak rf field on ^{1}H and, consequently, a relatively stronger rf field on ^{15}N during CP was applied to cover the ^{15}N chemical shift dispersion. A ^{15}N-^{1}H heteronuclear continuous-wave (CW) decoupling of 9.5 kHz was applied on the ^{1}H channel during the t_1 evolution period, whereas ^{15}N-^{1}H WALTZ decoupling with 13 μs pulse of RF field strength 18.9 kHz was applied on the ^{15}N channel during t_3. The phase-alternated HORROR sequence was applied for 8 ms duration with 35 kHz ^{1}H RF field. The γ-encoded symmetry-based pulse sequence $R18_8^7(270^\circ 90^\circ)$ was used for the ^{1}H CSA recoupling. The composite-180° pulse in each R element of $R18_8^7(270^\circ 90^\circ)$ pulse sequence is a combination of 270° and 90° RF pulses with corresponding phases alternating between (70°, 250°) and (-70°, -250°). The amplitude modulated t_2 signal was obtained at every $8\tau_r$ period. Delta NMR software (JEOL RESONANCE Inc.) was used to process all the NMR data. While a Fourier transformation after zero filling was applied in the t_1 and t_3 dimensions, a DC balance to remove DC offset effects (the average of the final 1/8th FID points in t_2 is subtracted from total data points) followed by zero filling and real Fourier transformation were applied in the CSA recoupling dimension (t_2) to process the 3D ^{15}N/^{1}H/^{1}H CS/CSA/CS correlation data. The CSA parameters were extracted through numerical fittings using SIMPSON program.[59] Powder averaging was achieved using 678 (α, β) crystal orientations and 26 γ angles.[60]

Results and Discussion

Molecular structure and 1D ^{1}H spectra of NAVL collected at 70 and 100 kHz MAS are shown in Figure 2. While the resolution and sensitivity are seen to be significantly improved for protons H3, H4, H5, H6 and H7 (peaks in the 0 - 6 ppm range) with increasing the MAS rate due to better suppression of ^{1}H/^{1}H homonuclear dipolar interactions, proton resonances from amide groups of Val and Leu remain unresolved even with a MAS rate as fast as 100 kHz. In other words, spectral resolution provided by 100 kHz MAS is not sufficient enough to resolve amide proton resonances with similar isotropic chemical shift values. This problem is crucial especially for the CSA measurement of structurally relevant protons from the 2D ^{1}H/^{1}H CSA/CS correlation experiments that require well-resolved ^{1}H resonances for the precise determination of CSA. To demonstrate this limitation further, we carried out 2D ^{1}H/^{1}H CSA/CS correlation measurement on NAVL at 70 kHz MAS.[23] Since CSA and heteronuclear dipolar coupling have the same spatial and spin symmetry, the previously reported pulse sequence simultaneously recouples both interactions. Subsequently, in order to accomplish ^{15}N-^{1}H heteronuclear decoupling such that any recoupling of heteronuclear dipolar interactions is avoided, we applied a 180° pulse on the ^{15}N channel in the middle of the CSA recoupling pulses. It is to be noted that NH proton CSA can also be measured in natural abundant samples wherein ^{14}N-^{1}H heteronuclear interactions are decoupled through on-resonance ^{14}N CW irradiation at ultrafast MAS.[45] The fast MAS spectrum of NAVL (Figure 3A) shows well-resolved resonances barring NH peaks, as a result CSA of amide protons cannot be determined. While the 2D ^{1}H/^{1}H CSA/CS correlation spectrum fails to provide any site-specific information about CSA of amide protons of NAVL, it can still be used to extract CSA of OH proton of –COOH group in NAVL. A spectral slice taken parallel to CSA dimension at the ^{1}H isotropic chemical shift of OH resonance is simulated using

SIMPSON[59] (Figure 3B) and ^{1}H CSA parameters obtained from the line shape fitting are: δaniso = δ_{zz}-δ_{iso} = 19.1 ppm and η = (δ_{yy}-δ_{xx})/δaniso = 0.3. Here, δ_{iso} is the isotropic chemical shift calculated using the relation (δ_{xx}+δ_{yy}+δ_{zz})/3, and the principal components of the chemical shift tensor (δ_{xx}, δ_{yy} and δ_{zz}) are defined as $|\delta_{zz}-\delta_{iso}| \geq |\delta_{xx}-\delta_{iso}| \geq |\delta_{yy}-\delta_{iso}|$.

The straightforward solution to overcome the issue of overlapping ^{1}H resonances of amide groups of NAVL is to carry out CSA measurement in a 3D manner by adding a high-resolution ^{15}N dimension so as to get well-resolved ^{15}N/^{1}H correlations. To this end, we implemented 3D ^{15}N/^{1}H/^{1}H CS/CSA/CS pulse sequence shown in Figure 1 to obtain amide proton CSA of Val and Leu residues of NAVL. As discussed earlier, ^{15}N chemical shifts are allowed to evolve during the incrementable t_1 period, and ^{15}N filtered ^{1}H signal after the two CP steps then evolves under recoupled ^{1}H CSA during the t_2 period in the absence of ^{15}N-^{1}H heteronuclear couplings. The 2D F1/F3 (^{15}N/^{1}H CS/CS) projection (Figure 4B) extracted from the 3D ^{15}N/^{1}H/^{1}H CS/CSA/CS spectrum of NAVL (Figure 4A) shows well-separated ^{15}N/^{1}H chemical shift correlations for Val and Leu residues of NAVL. Additionally, ^{1}H isotropic chemical shifts of amide protons are more precisely determined and can be used for the structural refinement using the quantum chemical calculations. To determine CSA of amide protons, the 2D F1/F2 (^{15}N/^{1}H CS/CSA) projection (Figure 5A) was extracted as the first step from the 3D ^{15}N/^{1}H/^{1}H CS/CSA/CS spectrum of NAVL (Figure 4A). In the subsequent step, spectral slices were taken parallel to the ^{1}H CSA dimension of the 2D F1/F2 (^{15}N/^{1}H CS/CSA) projection at the ^{15}N isotropic chemical shifts of Val and Leu residues of NAVL (Figure 5A). Finally, numerical simulations were performed to get the best fit of experimental ^{1}H CSA lineshapes (Figure 5B). The ^{1}H chemical shift parameters obtained are as follows: Val (δ_{iso} = 9.0 ppm, δaniso = 9.1 ppm, η = 0.7) and Leu (δ_{iso} = 9.2 ppm, δaniso = 9.1 ppm, η = 0.7). While we observed similar CSA parameters for the amide protons of NAVL, 3D ^{15}N/^{1}H/^{1}H CS/CSA/CS correlation experiment presented in this study is necessary for the cases where CSA of amide protons with unresolved peaks in the proton CS dimension are different and in principle leads to a direct correlation between ^{1}H CSA and ^{1}H CS. Subsequently, a set of CS and CSA of each amide proton can be extracted simultaneously.

Conclusion

In summary, we have presented a proton-detected 3D ^{15}N/^{1}H/^{1}H CS/CSA/CS correlation experiment at fast MAS (70 kHz) on NAVL. The main objective of this experiment is to determine site-resolved ^{1}H CSA of overlapped amide proton resonances through ^{15}N isotropic chemical shifts. The measured CSA parameters of amide protons of Val and Leu residues of NAVL are found to be identical. In addition, we have also reported ^{1}H CSA of well-resolved OH resonance of NAVL obtained from 2D ^{1}H/^{1}H CSA/CS correlation experiment. We believe that the proton-detected 3D pulse sequence presented in this study can be implemented for studies relying on ^{1}H CSAs in more complex chemical and biological systems wherein a limited or no resolution is a major problem to overcome. Additionally, a combination of partially-deuterated samples, higher magnetic field, and faster spinning speed (>100 kHz) can further reduce the difficulties due to spectral resolution from macromolecular systems.[26,31,34,61,62]

Acknowledgments

This work was supported by the funds from National Institutes of Health (GM084018 and GM095640 to A. R.).

References

1. Cornilescu G, Bax A. Measurement of Proton, Nitrogen, and Carbonyl Chemical Shielding Anisotropies in a Protein Dissolved in a Dilute Liquid Crystalline Phase. J Am Chem Soc. 2000; 122:10143–10154.
2. Tjandra N, Bax A. Solution NMR Measurement of Amide Proton Chemical Shift Anisotropy in ^{15}N-Enriched Proteins. Correlation with Hydrogen Bond Length. J Am Chem Soc. 1997; 119:8076–8082.
3. Tjandra N, Bax A. Large Variations in ^{13}C(Alpha) Chemical Shift Anisotropy in Proteins Correlate with Secondary Structure. J Am Chem Soc. 1997; 119:9576–9577.
4. Yao LS, Grishaev A, Cornilescu G, Bax A. The Impact of Hydrogen Bonding on Amide ^{1}H Chemical Shift Anisotropy Studied by Cross-Correlated Relaxation and Liquid Crystal NMR Spectroscopy. J Am Chem Soc. 2010; 132:10866–10875. [PubMed: 20681720]
5. Yao LS, Grishaev A, Cornilescu G, Bax A. Site-Specific Backbone Amide ^{15}N Chemical Shift Anisotropy Tensors in a Small Protein from Liquid Crystal and Cross-Correlated Relaxation Measurements. J Am Chem Soc. 2010; 132:4295–4309. [PubMed: 20199098]
6. Wu G, Freure CJ, Verdurand E. Proton Chemical Shift Tensors and Hydrogen Bond Geometry: A ^{1}H-^{2}H Dipolar NMR Study of the Water Molecule in Crystalline Hydrates. J Am Chem Soc. 1998; 120:13187–13193.
7. Wei YF, de Dios AC, McDermott AE. Solid-State ^{15}N NMR Chemical Shift Anisotropy of Histidines: Experimental and Theoretical Studies of Hydrogen Bonding. J Am Chem Soc. 1999; 121:10389–10394.
8. Pandey MK, Vivekanandan S, Ahuja S, Pichumani K, Im SC, Waskell L, Ramamoorthy A. Determination of ^{15}N Chemical Shift Anisotropy from a Membrane-Bound Protein by NMR Spectroscopy. J Phys Chem B. 2012; 116:7181–7189. [PubMed: 22620865]
9. Pandey MK, Vivekanandan S, Ahuja S, Huang R, Im SC, Waskell L, Ramamoorthy A. Cytochrome-P450-Cytochrome-b_5 Interaction in a Membrane Environment Changes ^{15}N Chemical Shift Anisotropy Tensors. J Phys Chem B. 2013; 117:13851–13807. [PubMed: 24107224]
10. Pandey MK, Ramamoorthy A. Quantum Chemical Calculations of Amide-^{15}N Chemical Shift Anisotropy Tensors for a Membrane-Bound Cytochrome-b5. J Phys Chem B. 2013; 117:859–867. [PubMed: 23268659]
11. Lee DK, Wittebort RJ, Ramamoorthy A. Characterization of ^{15}N Chemical Shift and ^{1}H-^{15}N Dipolar Coupling Interactions in a Peptide Bond of Uniaxially Oriented and Polycrystalline Samples by One-Dimensional Dipolar Chemical Shift Solid-State NMR Spectroscopy. J Am Chem Soc. 1998; 120:8868–8874.
12. Loth K, Pelupessy P, Bodenhausen G. Chemical Shift Anisotropy Tensors of Carbonyl, Nitrogen, and Amide Proton Nuclei in Proteins through Cross-Correlated Relaxation in NMR Spectroscopy. J Am Chem Soc. 2005; 127:6062–6068. [PubMed: 15839707]
13. Gerald R, Bernhard T, Haeberlen U, Rendell J, Opella S. Chemical-Shift and Electric-Field Gradient Tensors for the Amide and Carboxyl Hydrogens in the Model Peptide N-Acetyl-D,L-Valine - Single-Crystal Deuterium NMR-Study. J Am Chem Soc. 1993; 115:777–782.
14. Duma L, Abergel D, Tekely P, Bodenhausen G. Proton Chemical Shift Anisotropy Measurements of Hydrogen-Bonded Functional Groups by Fast Magic-Angle Spinning Solid-State NMR Spectroscopy. Chem Commun. 2008:2361–2363.
15. Hou GJ, Paramasivam S, Yan S, Polenova T, Vega AJ. Multidimensional Magic Angle Spinning NMR Spectroscopy for Site-Resolved Measurement of Proton Chemical Shift Anisotropy in Biological Solids. J Am Chem Soc. 2013; 135:1358–1368. [PubMed: 23286322]
16. Hou GJ, Gupta R, Polenova T, Vega AJ. A Magic-Angle-Spinning NMR Spectroscopy Method for the Site-Specific Measurement of Proton Chemical-Shift Anisotropy in Biological and Organic Solids. Isr J Chem. 2014; 54:171–183. [PubMed: 25484446]

17. Hou GJ, Byeon IJL, Ahn J, Gronenborn AM, Polenova T. Recoupling of Chemical Shift Anisotropy by R-Symmetry Sequences in Magic Angle Spinning NMR Spectroscopy. J Chem Phys. 2012; 137
18. Miah HK, Bennett DA, Iuga D, Titman JJ. Measuring Proton Shift Tensors with Ultrafast MAS NMR. J Magn Reson. 2013; 235:1–5. [PubMed: 23911900]
19. Brouwer DH, Ripmeester JA. Symmetry-Based Recoupling of Proton Chemical Shift Anisotropies in Ultrahigh-Field Solid-State NMR. J Magn Reson. 2007; 185:173–178. [PubMed: 17188919]
20. Wu CH, Ramamoorthy A, Gierasch LM, Opella SJ. Simultaneous Characterization of the Amide ^{1}H Chemical Shift, ^{1}H-^{15}N Dipolar, and ^{15}N Chemical-Shift Interaction Tensors in a Peptide-Bond by 3-Dimensional Solid-State NMR-Spectroscopy. J Am Chem Soc. 1995; 117:6148–6149.
21. Sack I, Macholl S, Wehrmann F, Albrecht J, Limbach HH, Fillaux F, Baron MH, Buntkowsky G. A ^{15}N-^{1}H Dipolar CSA Solid-State NMR Study of (-CO-CD2-^{15}NH-)$_n$. Appl Magn Reson. 1999; 17:413–431.
22. Hou G, Paramasivam S, Byeon IJ, Gronenborn AM, Polenova T. Determination of Relative Tensor Orientations by Gamma-Encoded Chemical Shift Anisotropy/Heteronuclear Dipolar Coupling 3D NMR Spectroscopy in Biological Solids. Phys Chem chem Phys. 2010; 12:14873–14883. [PubMed: 20936218]
23. Pandey MK, Malon M, Ramamoorthy A, Nishiyama Y. Composite-180° Pulse-Based Symmetry Sequences to Recouple Proton Chemical Shift Anisotropy Tensors under Ultrafast MAS Solid-State NMR Spectroscopy. J Magn Reson. 2015; 250:45–54. [PubMed: 25497846]
24. Pandey MK, Nishiyama Y. Determination of Relative Orientation between ^{1}H CSA Tensors from a 3D Solid-State NMR Experiment Mediated through ^{1}H/^{1}H RFDR Mixing under Ultrafast MAS. Solid State Nucl Magn Reson. 2015; 70:15–20. [PubMed: 26065628]
25. Ishii Y, Tycko R. Sensitivity Enhancement in Solid State ^{15}N NMR by Indirect Detection with High-Speed Magic Angle Spinning. J Magn Reson. 2000; 142:199–204. [PubMed: 10617453]
26. Wickramasinghe A, Wang S, Matsuda I, Nishiyama Y, Nemoto T, Endo Y, Ishii Y. Evolution of CPMAS under Fast Magic-Angle-Spinning at 100 kHz and Beyond. Solid State Nucl Magn Reson. 2015; doi: 10.1016/j.ssnmr.2015.10.002
27. Pandey MK, Nishiyama Y. Proton-Detected 3D ^{14}N/^{14}N/^{1}H Isotropic Shift Correlation Experiment Mediated through ^{1}H-^{1}H RFDR Mixing on a Natural Abundant Sample under Ultrafast MAS. J Magn Reson. 2015; 258:96–101. [PubMed: 26232769]
28. Mroue K, Nishiyama Y, Pandey MK, Gong B, McNerny E, Kohn D, Morris M, Ramamoorthy A. Proton-Detected Solid-State NMR Spectroscopy of Bone with Ultrafast Magic Angle Spinning. Scientific Reports. 2015; 5:11991. [PubMed: 26153138]
29. Zhang R, Pandey MK, Nishiyama Y, Ramamoorthy A. A Novel High-Resolution and Sensitivity-Enhanced Three-Dimensional Solid-State NMR Experiment under Ultrafast Magic Angle Spinning Conditions. Scientific Reports. 2015; 5:11810. [PubMed: 26138791]
30. Asami S, Rakwalska-Bange M, Carlomagno T, Reif B. Protein-Rna Interfaces Probed by 1h-Detected MAS Solid-State NMR Spectroscopy. Angew Chem. 2013; 52:2345–2349. [PubMed: 23335059]
31. Asami S, Reif B. Proton-Detected Solid-State NMR Spectroscopy at Aliphatic Sites: Application to Crystalline Systems. Acc Chem Res. 2013; 46:2089–2097. [PubMed: 23745638]
32. Asami S, Schmieder P, Reif B. High Resolution 1H-detected Solid-State NMR Spectroscopy of Protein Aliphatic Resonances: Access to Tertiary Structure Information. J Am Chem Soc. 2010; 132:15133–15135. [PubMed: 20939587]
33. Huber M, Hiller S, Schanda P, Ernst M, Bockmann A, Verel R, Meier BH. A Proton-Detected 4D Solid-State NMR Experiment for Protein Structure Determination. ChemPhysChem. 2011; 12:915–918. [PubMed: 21442705]
34. Barbet-Massin E, Pell AJ, Retel JS, Andreas LB, Jaudzems K, Franks WT, Nieuwkoop AJ, Hiller M, Higman V, Guerry P, Bertarello A, Knight MJ, Felletti M, Le Marchand T, Kotelovica S, Akopjana I, Tars K, Stoppini M, Bellotti V, Bolognesi M, Ricagno S, Chou JJ, Griffin RG, Oschkinat H, Lesage A, Emsley L, Herrmann T, Pintacuda G. Rapid Proton-Detected NMR Assignment for Proteins with Fast Magic Angle Spinning. J Am Chem Soc. 2014; 136:12489–12497. [PubMed: 25102442]

35. Kobayashi T, Mao K, Paluch P, Nowak-Krol A, Sniechowska J, Nishiyama Y, Gryko DT, Potrzebowski MJ, Pruski M. Study of Intermolecular Interactions in the Corrole Matrix by Solid-State NMR under 100 KHz MAS and Theoretical Calculations. Angew Chem. 2013; 52:14108–14111. [PubMed: 24227750]
36. Nishiyama Y, Endo Y, Nemoto T, Utsumi H, Yamauchi K, Hioka K, Asakura T. Very Fast Magic Angle Spinning ^{1}H-^{14}N 2d Solid-State NMR: Sub-Micro-Liter Sample Data Collection in a Few Minutes. J Magn Reson. 2011; 208:44–48. [PubMed: 21035366]
37. Nishiyama Y, Malon M, Ishii Y, Ramamoorthy A. 3D ^{15}N/^{15}N/^{1}H Chemical Shift Correlation Experiment Utilizing an RFDR-Based ^{1}H/^{1}H Mixing Period at 100 KHz MAS. J Magn Reson. 2014; 244:1–5. [PubMed: 24801998]
38. Takeda K. Microcoils and Microsamples in Solid-State NMR. Solid State Nucl Magn Reson. 2012; 47-48:1–9. [PubMed: 23083521]
39. Hoult DI, Richards RE. Signal-to-Noise Ratio of Nuclear Magnetic-Resonance Experiment. J Magn Reson. 1976; 24:71–85.
40. Minard KR, Wind RA. Solenoidal Microcoil Design. Part I: Optimizing RF Homogeneity and Coil Dimensions. Concept Magnetic Res. 2001; 13:128–142.
41. Minard KR, Wind RA. Solenoidal Microcoil Design - Part II: Optimizing Winding Parameters for Maximum Signal-to-Noise Performance. Concept Magnetic Res. 2001; 13:190–210.
42. Janssen H, Brinkmann A, van Eck ERH, van Bentum PJM, Kentgens APM. Microcoil High-Resolution Magic Angle Spinning NMR Spectroscopy. J Am Chem Soc. 2006; 128:8722–8723. [PubMed: 16819853]
43. Kentgens APM, Bart J, van Bentum PJM, Brinkmann A, Van Eck ERH, Gardeniers JGE, Janssen JWG, Knijn P, Vasa S, Verkuijlen MHW. High-Resolution Liquid- and Solid-State Nuclear Magnetic Resonance of Nanoliter Sample Volumes Using Microcoil Detectors. J Chem Phys. 2008; 128
44. Sakellariou D, Le Goff G, Jacquinot JF. High-Resolution, High-Sensitivity NMR of Nanolitre Anisotropic Samples by Coil Spinning. Nature. 2007; 447:694–697. [PubMed: 17554303]
45. Pandey MK, Nishiyama Y. Determination of NH Proton Chemical Shift Anisotropy with ^{14}N-^{1}H Heteronuclear Decoupling Using Ultrafast Magic Angle Spinning Solid-State NMR. J Magn Reson. 2015; doi: 10.1016/j.jmr.2015.10.015
46. Ernst M, Samoson A, Meier BH. Low-Power Decoupling in Fast Magic-Angle Spinning NMR. Chem Phys Lett. 2001; 348:293–302.
47. Meier BH. Cross Polarization under Fast Magic Angle Spinning - Thermodynamical Considerations. Chem Phys Lett. 1992; 188:201–207.
48. Lange A, Scholz I, Manolikas T, Ernst M, Meier BH. Low-Power Cross Polarization in Fast Magic-Angle Spinning NMR Experiments. Chem Phys Lett. 2009; 468:100–105.
49. Laage S, Marchetti A, Sein J, Pierattelli R, Sass HJ, Grzesiek S, Lesage A, Pintacuda G, Emsley L. Band-Selective 1H-13C Cross-Polarization in Fast Magic Angle Spinning Solid-State NMR Spectroscopy. J Am Chem Soc. 2008; 130:17216–17217. [PubMed: 19053413]
50. Amoureux JP, Pruski M. Theoretical and Experimental Assessment of Single- and Multiple-Quantum Cross-Polarization in Solid State NMR. Mol Phys. 2002; 100:1595–1613.
51. Metz G, Wu XL, Smith SO. Ramped-Amplitude Cross-Polarization in Magic-Angle-Spinning NMR. J Magn Reson Ser A. 1994; 110:219–227.
52. Levitt MH, Oas TG, Griffin RG. Rotary Resonance Recoupling in Heteronuclear Spin Pair Systems. Isr J Chem. 1988; 28:271–282.
53. Oas TG, Griffin RG, Levitt MH. Rotary Resonance Recoupling of Dipolar Interactions in Solid-State Nuclear Magnetic-Resonance Spectroscopy. J Chem Phys. 1988; 89:692–695.
54. Nielsen NC, Bildsoe H, Jakobsen HJ, Levitt MH. Double-Quantum Homonuclear Rotary Resonance - Efficient Dipolar Recovery in Magic-Angle-Spinning Nuclear-Magnetic-Resonance. J Chem Phys. 1994; 101:1805–1812.
55. Ishii Y, Yesinowski JP, Tycko R. Sensitivity Enhancement in Solid-State ^{13}C NMR of Synthetic Polymers and Biopolymers by ^{1}H NMR Detection with High-Speed Magic Angle Spinning. J Am Chem Soc. 2001; 123:2921–2922. [PubMed: 11456995]

56. Hou GJ, Lu XY, Vega AJ, Polenova T. Accurate Measurement of Heteronuclear Dipolar Couplings by Phase-Alternating R-Symmetry (PARS) Sequences in Magic Angle Spinning NMR Spectroscopy. J Chem Phys. 2014; 141
57. Marion D, Ikura M, Tschudin R, Bax A. Rapid Recording of 2D NMR-Spectra without Phase Cycling - Application to the Study of Hydrogen-Exchange in Proteins. J Magn Reson. 1989; 85:393–399.
58. Pandey MK, Qadri Z, Ramachandran R. Understanding Cross-Polarization (CP) NMR Experiments through Dipolar Truncation. J Chem Phys. 2013; 138
59. Bak M, Rasmussen JT, Nielsen NC. Simpson: A General Simulation Program for Solid-State NMR Spectroscopy. J Magn Reson. 2000; 147:296–330. [PubMed: 11097821]
60. Bak M, Nielsen NC. Repulsion, a Novel Approach to Efficient Powder Averaging in Solid-State NMR. J Magn Reson. 1997; 125:132–139. [PubMed: 9245368]
61. Pandey, MK.; Zhang, R.; Hashi, K.; Ohki, S.; Nishijima, G.; Matsumoto, S.; Noguchi, T.; Deguchi, K.; Goto, A.; Shimizu, T.; Maeda, H.; Takahashi, M.; Yanagisawa, Y.; Yamazaki, T.; Iguchi, S.; Tanaka, R.; Nemoto, T.; Miyamoto, T.; Suematsu, H.; Saito, K.; Miki, T.; Ramamoorthy, A.; Nishiyama, Y. 1020 Mhz Single-Channel Proton Fast Magic Angle Spinning Solid-State NMR Spectroscopy. J Magn Reson. 2015. DOI: http://dx.doi.org/10.1016/j.jmr.2015.10.003
62. Bertini I, Emsley L, Lelli M, Luchinat C, Mao J, Pintacuda G. Ultrafast MAS Solid-State NMR Permits Extensive ^{13}C and ^{1}H Detection in Paramagnetic Metalloproteins. J Am Chem Soc. 2010; 132:5558–5559. [PubMed: 20356036]

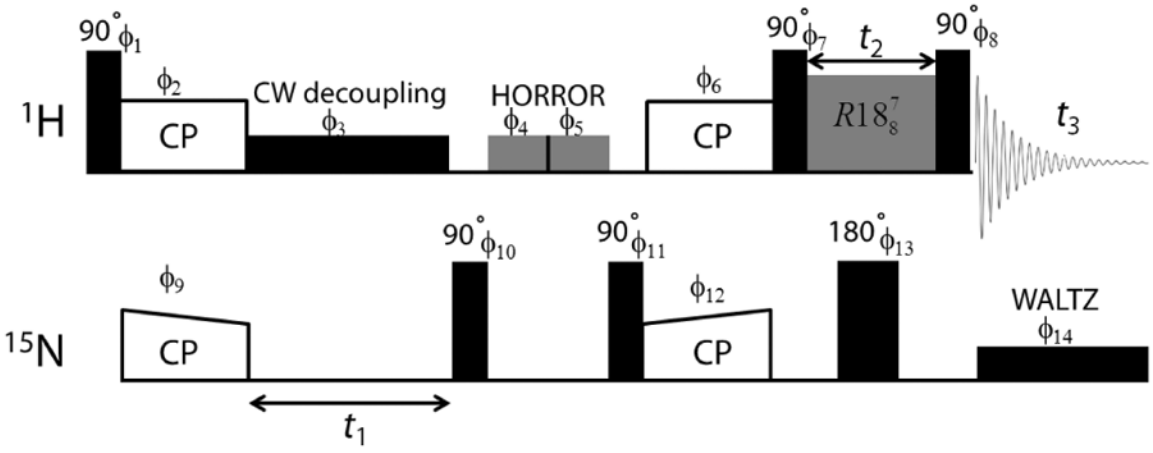

Figure 1.

Proton-detected 3D $^{15}N/^{1}H/^{1}H$ CS/CSA/CS pulse sequence. ^{15}N chemical shifts are expressed during t_1 under the low-power ^{1}H CW decoupling, while ^{1}H CSAs are recoupled during t_2. Simultaneous recoupling of ^{15}N-^{1}H hetronuclear interactions are avoided by the application of 180° pulse on the ^{15}N channel in the middle of CSA recoupling pulses. The phase cycling scheme used in the 3D pulse sequence is as follows: φ_1 = {4 (0), 4 (180)}, φ_2 = {90}, φ_3 = {0}, φ_4 = {0}, φ_5 = {90}, φ_6 = {2 (0), 2 (180)}, φ_7 = {90}, φ_8 = {270}, φ_9 = {{0, 180}, {90, 270}}, φ_{10}= {90}, φ_{11} = {270}, φ_{12} = {0}, φ_{13} = {0}, φ_{14} = {0}, φ_{acq} = {0, 180, 180, 0, 180, 0, 0, 180}.

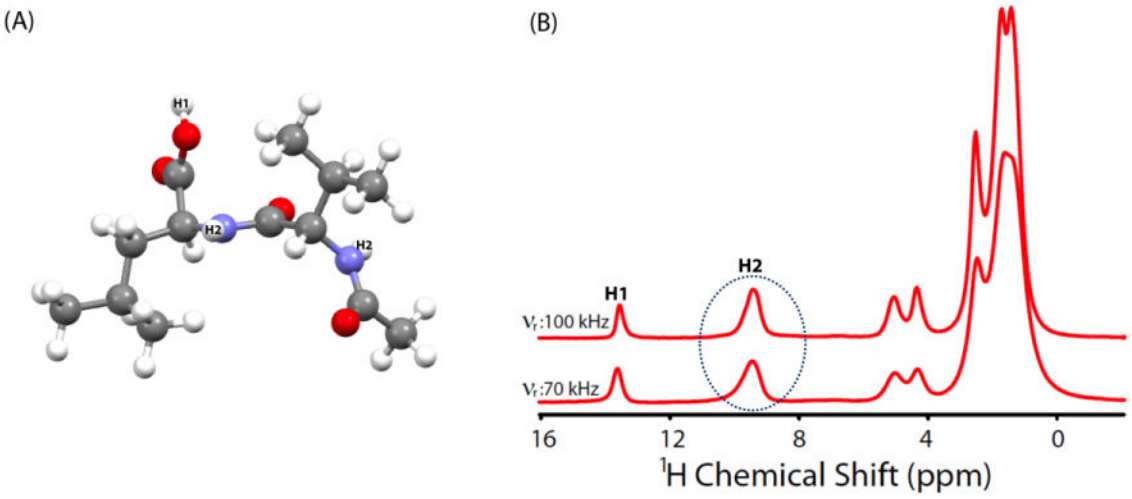

Figure 2.

Molecular structure and ^{1}H NMR spectra of a powder sample of NAVL recorded at 600 MHz under 70 and 100 kHz MAS frequencies.

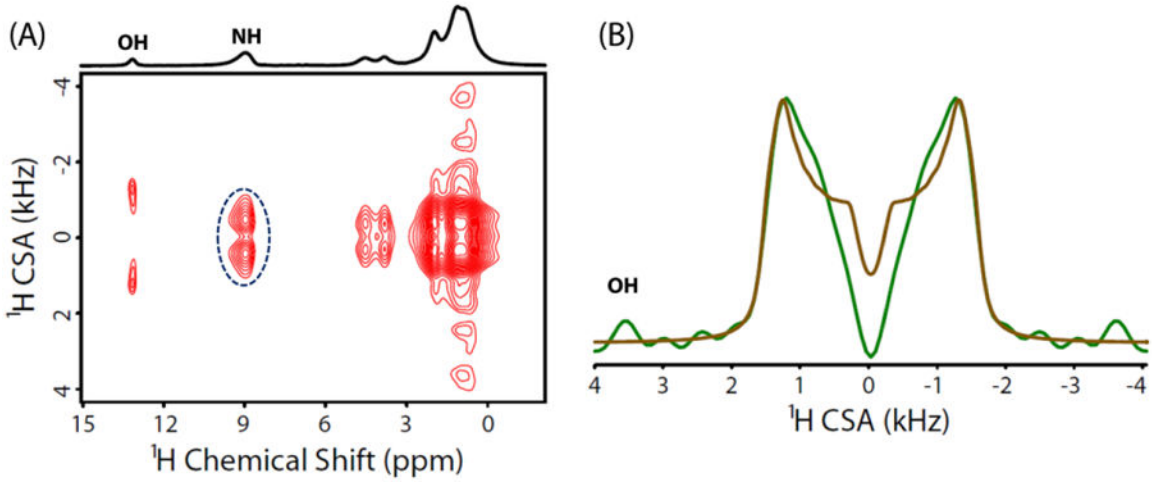

Figure 3.

(A) Two-dimensional ^{1}H/^{1}H CSA/CS correlation spectrum of NAVL at 600 MHz under 70 kHz MAS obtained using a previously reported pulse sequence[23] with a 180° pulse in the middle of the CSA recoupling period on the ^{15}N channel to decouple ^{15}N-^{1}H heteronuclear interactions. In the 2D ^{1}H/^{1}H CSA/CS correlation experiment 6 scans were collected every 32 t_1 increments and a recycle delay of 5 s was used (total experimental time = 16 minutes). Dotted circle indicates the two overlapped amide proton resonances. (B) The experimental CSA lineshape extracted by taking a slice (green line) parallel to the ^{1}H CSA dimension of the 2D spectrum at the ^{1}H isotropic chemical shift frequency of OH resonance of NAVL. Best fitting simulated lineshape (brown) was obtained using SIMPSON simulations.

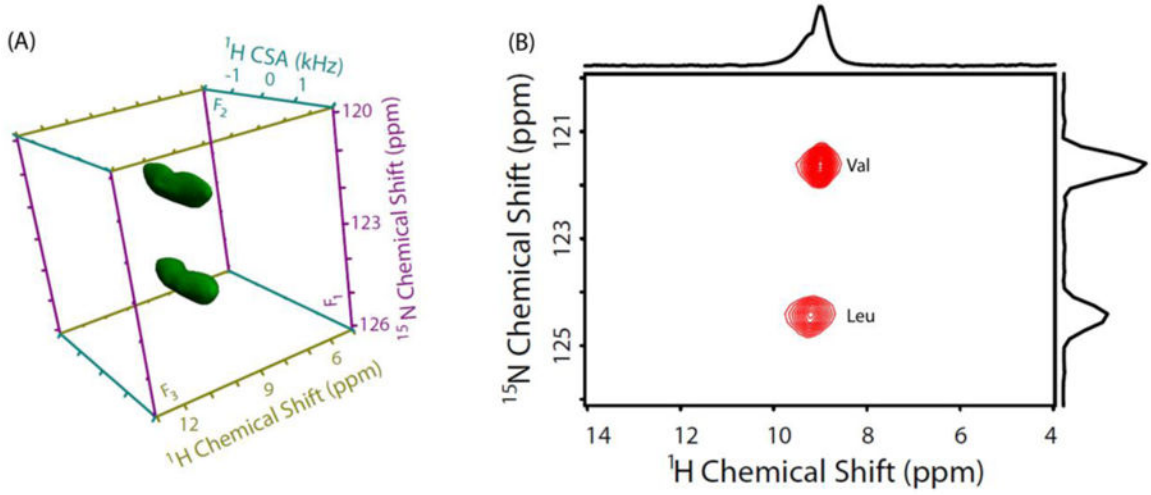

Figure 4.

(A) 3D ^{15}N/^{1}H/^{1}H CS/CSA/CS correlation spectrum of NAVL at 70 kHz MAS frequency. (B) 2D F1/F3 (^{15}N/^{1}H CS/CS) projection extracted from the 3D ^{15}N/^{1}H/^{1}H CS/CSA/CS spectrum of NAVL. Total experimental time = 22.5 hours.

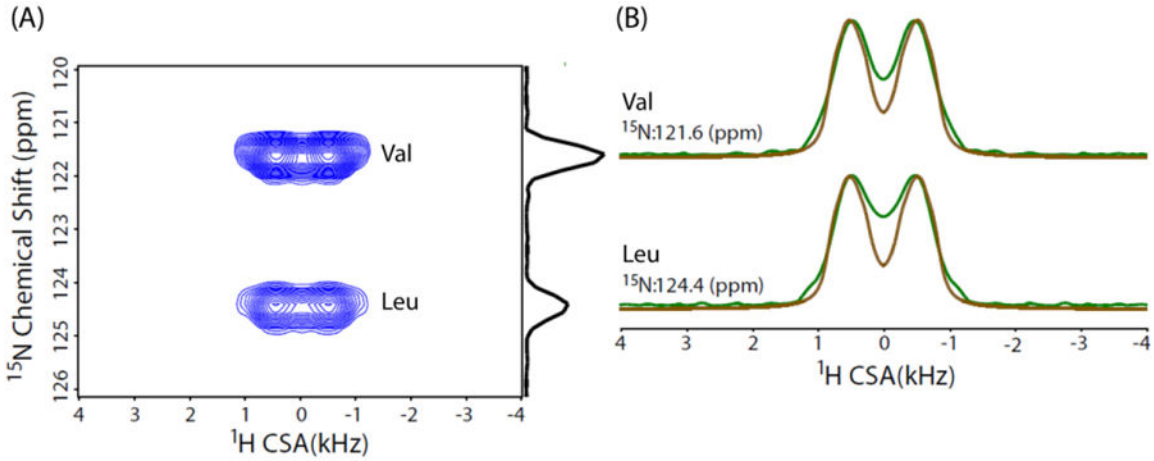

Figure 5.

(A) Two-dimensional F1/F2 (^{15}N/^{1}H CS/CSA) projection extracted from the 3D ^{15}N/^{1}H/^{1}H CS/CSA/CS spectrum of NAVL. (B) Spectral slices (green) taken parallel to the ^{1}H CSA dimension at the ^{15}N chemical shifts of Val and Leu residues of NAVL, and corresponding simulated lineshapes (brown).